CrystEngComm

Accepted Manuscript

ROYAL SOCIETY OF CHEMISTRY

www.rsc.org/crystengcomm

New insight into Size-Controlled Synthesis of Silver Nanoparticles and Its Superiority in Room Temperature Sintering

Yao Tang, Wei He*, Shouxu Wang, Zhihua Tao, Lijuan Cheng

For the better application of room-temperature sintering in printed electronics, a low-cost and convenient approach to synthesize size-controlled silver nanoparticles (Ag NPs) with ca. 37 nm in average diameter is presented. Monodisperse Ag NPs with narrow size distribution were rapidly and routinely produced on relatively large scales through a typical polyol process using poly(vinyl pyrrolidone) (PVP) as capping agent, poly(ethylene glycol) (PEG) to enhance the reducibility and viscosity of solvent. These Ag NPs would suffer a spontaneous sintering, which was triggered by desorption of PVP from their surface, when they encountered a certain amount of Cl^-; the eventual coalescence and Ostwald ripening processes would make their structure more compact and solider, leading to a high conductivity even up to 40% that of bulk silver.

Introduction

In recent years printed electronics have caused widespread concern by using a low cost, low pollution and convenient way to produce electronic device instead of conventional technology. Conductive inks play an important part in this field and even could influence the development of the whole industry. Nowadays, many kinds of conductive inks have been developed with the progress in synthesis of various nano material.[1-6] Among all the metals, silver presents high electrical conductivity, stability and is easy to be controlled in size or shape during synthesis. Hence silver inks have been extensively developed for their wide potential applications in all sorts of electron devices such as radio frequency identification (RFID), photovoltaics, electrical circuits, sensors, displays, etc.[7-11] In order to lower cost and expand application, the conductive inks need to be printed on all sorts of substrates, especially on some flexible substrates such as paper and polymer film instead of the expensive traditional materials.[12-16] As these substrates are temperature sensitive, they require a relative low sintering temperature to prevent destruction by heating. But it is a hard work for most of conductive inks to realize sintering blow 90℃ by heating.[17-21] In addition, metal nanoparticles dispersed in conductive inks are also easy to be oxidized by heating in air, losing conductivity. Therefore, conventional sintering is not the best way to be applied in those situations.

Some new sintering techniques including microwave sintering, laser radiation sintering, electrical sintering etc., have been developed in order to avoid the disadvantages.[22-26] But these techniques rely on some advanced apparatus, which are exceptionally expensive and have complex manipulation, blocking their way to practical application. In recent years, Shlome Magdassi et al. found a new convenient approach to sinter their silver ink at room temperature by a chemical process, which was a successful substitute for conventional technology.[27,28] They introduced a new conception by stabilizing silver nanoparticles (Ag NPs) with poly(acrylic acid) sodium salt (PAA Na) in dispersion before use, then destabilizing them by some anions during application, leading to a spontaneous coalescence between particles to realize sintering. It made the sintering of Ag NPs at room temperature possible and also simplified sintering procedure. On this basis we have found Poly(vinyl pyrrolidone) (PVP) was competent to stabilize Ag NPs by adsorbing on their surface and could be facilely detached by Cl^-, also leading to the spontaneous sintering process.[29] This sintering in fact is dependent on two spontaneous behaviors of Ag NPs after they have been destabilized, i.e. coalescence and Ostwald ripening.[30,31] It was found in our experiment that these two behaviors could be extremely affected by the size of Ag NPs, which consequently influenced the level of sintering. The large Ag NPs synthesized by our previous recipe did not perform very well in the chemical process, leaving a lot of room for improving.

A new approach based on our former works to synthesize size-controlled Ag NPs for the application of room-temperature sintering is reported in this paper. Silver nitrate (AgNO3) was reduced by the mixture of ethylene glycol (EG) and poly(ethylene glycol) (PEG) in the presence of PVP. Different ratios of PEG/EG have been evaluated; it was found when the ratio of PEG/EG reached ca. 2:1 small Ag NPs with average size blow 40 nm would be produced in high yield. Comparing with our previous Ag NPs ca. 100 nm in size, these small Ag NPs presented great superiority in room temperature sintering. The silver patterns fabricated with the small Ag NPs also reached a high conductivity after sintering, even up to 40% that of bulk silver. The possible reasons behind those

phenomena and the corresponding mechanisms are discussed with various characterizations.

Experimental

Materials

All the chemical reagents used in the experiments were purchased from commercial sources and used without further purification. Anhydrous ethanol(CH3CH2OH, 99.7%), EG (99.6%), AgNO3 (99.8%), sodium chloride (NaCl, 99%), hydrochloric acid (HCl, 36%～38%) PEG (Mw≈400) and PVP (Mw≈30 000) were purchased from KELONG Chemical Company, Chengdu, China. The substrates were offered by Shengyi Technology Co. Ltd. The deionized water was obtained from an ion exchange system.

Synthesis of Ag NPs

The small Ag NPs were prepared by a polyol process as follow: 100 mg of AgNO3 and 130 mg of PVP were both dissolved in 10 mL EG. Then 20 mL PEG was added into the solution. After that, the mixture was placed in a flask, heated and thermally stabilized at 140℃ with continuous magnetic stirring for ca. 5 min. According to this ratio of PEG/EG, the reaction almost accomplished in 3~5 min; and if the reaction was allowed to continue, most Ag NPs would start to aggregate. After reaction, the resulting mixture was naturally cooled to room temperature, and diluted with anhydrous ethanol (5~10 times by volume), centrifuged at 8000 rpm for ca. 20 min. Supernatant containing impurity and residua of reagent could be easily removed using a pipette. This procedure was repeated several times till the supernatant became transparent. Finally, the Ag NPs were redispersed in deionized water according to the ratio of 15wt% for characterization and further use. In order to investigate the effect of PEG on size control of Ag NPS, mixtures of PEG and EG were used for synthesis according to a series of ratios (including 5:1, 2:1, 1:1, 1:2, 1:5). In order to facilitate comparison, these experiments were carried out under the same condition, using the preceding procedures and keeping the sum volume of PEG and EG constant; all the reactions were only allowed to last 5 min though it was not long enough for the last two sets experiments, it could offered enough evidences for judgment.

Room temperature sintering

To make the patterns fabricated by the Ag NPs to be conductive, it entails a sintering procedure which could lead to the close contact and coalescence of particles. The chemical process operated at room temperature was used instead of conventionally sintering by heating. Firstly, an experiment, which could indirectly verify the feasibility of room temperature sintering process, was carried out based on the liquid phase reaction of Ag NPs and HCl. One drop of HCl (0.1M) was added into the dispersion of Ag NPs; and the whole deposition course of Ag NPs was recorded by a digital camera (Fujifilm, FinePix Z3). That sample was compared with the original one through the whole reaction. In order to illustrate the superiority of the size-controlled Ag NPs in sintering, two silver traces were fabricated on FR-4 substrate by a semi-automatic screen printing (Lenstar, BH-7010) respectively using size-controlled Ag NPs and original large ones. After solidification, these traces were immersed into hydrochloric acid (0.1M) and sonicated by an ultrasonic cleaner (As3120) for ca. 90 min. After each 5 min, the sample was taken out, washed and recorded the resistivity during the chemical process.

Characterization

The scanning electron microscopy (SEM) and high-resolution transmission electron microscopy (HR-TEM) images were respectively obtained with scanning electron microscope (FEI, inspect F) operated at 80kV and field emission transmission electron microscope (Tecnai, G2 F20 S-TWIN) operated at 200kV. The x-ray diffraction (XRD) data were taken by a powder diffractometer (X' Pert Pro MPD) with Cu Kα radiation (λ=1.54Å). UV/vis absorption spectra were recorded by a Shimadzu UV-3600 spectrophotometer, with a 1 cm path length quartz cell. X-ray photoelectron spectroscopy (XPS) data were obtained by a Kratos XSAM 800 X-ray Photoelectron Spectrometer. Particle size distributions were recorded by a laser diffraction particle size analyzer (JL-1197). Resistivity of the silver traces was evaluated by calculation with resistance measured by a milliohm meter (NJ23-DMR-1) and thickness measured by microsection image of vertical section through a metaloscope (Nikon, ME-600). All photos were taken by a digital camera (Fujifilm, FinePix Z3).

Results and discussion

Comparing with our previous results (Ag NPs synthesized with ca. 100nm in diameter)[29], smaller nanoparticles (30~40 nm in diameter) were rapidly and routinely produced on relatively large scales only by adding an amount of PEG, because PEG can provide strong reducibility and high viscosity which are able to accelerate the reaction rate enhancing the efficiency of production of Ag NPs while preventing the particles from aggregation. In order to investigate the contribution of PEG to the restraint of particle size, different mixtures of PEG and EG with a series

of volume ratio including 5:1, 2:1, 1:1, 1:2 and 1:5 were used for prepare Ag NPs. Figure 1(A) shows the freshly prepared samples containing the same dosage of AgNO3 and PVP; only the ratios of PEG/EG are different which are listed on the top. It can be clearly seen that the mixture reflected an opaque milkiness at high ratio of PEG/EG, because PEG is not a good solvent for AgNO3 and PVP; them could not completely resolved in this mixture. Hence AgNO3 and PVP would better be dissolved in EG firstly, then add PEG and keep a ratio of PEG/EG blow 5:1. Figure 1(B) shows the reaction products which were obtained by heating the series of mixtures at 140℃ for 5 min. It seems that the samples with low ratio of PEG/EG produced a low concentration of Ag NPs; they are light in color and even appear a slight transparent, because the reducibility of the solvent becomes weaker with the decrease of PEG in dosage and it cannot yield so much Ag NPs at the given time.

Figure 1 (a-e) show a series of SEM images of Ag NPs that were respectively taken from the samples listed in figure 1(B). And the corresponding size distributions of particle were shown in figure 2 (a-e). Strangely, when the ratio of PEG/EG was 5:1, the yielded Ag NPs had the largest size and showed a wide distribution in diameter. From the SEM image it also can be seen some big irregular particles like ellipsoid or rice were mixed up with the spherical particles, indicating that there had occurred anisotropic growth and bad aggregation of Ag NPs during the synthesis; it is most probably attributed to the incomplete dissolution of reagents. In addition to this, PVP had not been dissolved completely; it could not well prevent the aggregation of Ag NPs. The high concentration of PEG enhanced the reducibility of solvent greatly. Hence those Ag NPs suffered a fast growth without restraining by PVP and grew anisotropically. When the ratio of PEG and EG was altered to 2:1, a dramatic change had happened. The obtained Ag NPs became much uniform, ca. 37nm in average diameter, close to spherical in shape and narrow distribution in size. (These characteristics would facilitate the redispersion of Ag NPs in other solvent to make further application such as preparing conductive inks.) This result bases on the complete dissolution of reagents, a high viscosity and strong reducing environment which will be discussed later. Besides the incomplete dissolution of reagents (PEG and EG in the ratio of 5:1), it could be found that the particles became larger with the decease of PEG. Since the ratio of PEG/EG decreased to 1:2, the solvent has appeared a weak reducibility leading to a low yield of Ag NPs. It could prolong the reaction time to produce more Ag NPs, but most of the particles would grow into even larger size. In figure 1d&e it also can be observed many irregular particles. It seems the anisotropic growth, aggregation and coalescence became severer to the particles. Many small particles which have not had enough time for growth also yielded due to the weak reducibility, resulting in a board distribution in size (figure 2d&e).

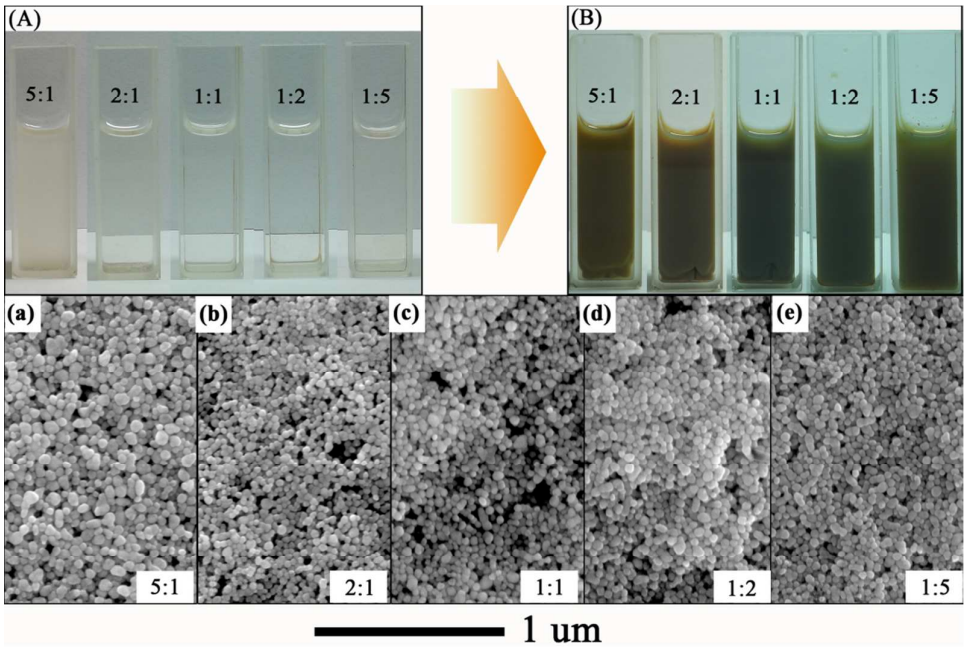

Fig. 1 (A) Photographs of freshly prepared precursor solution in the mixtures of PEG and EG with a series of volume ratio (the ratios of PEG/EG were listed on the top). (B) The products respectively obtained after heating the precursor solution at 140℃ for 5 min. (a-e) SEM images of Ag NPs respectively taken from the samples of these mixtures listed in (B).

Figure 2f shows the UV-vis extinction spectra of the Ag NPs respectively recorded from the resulting mixtures (figure 2B) diluted 1000 times with ethanol. The intensity of absorption peaks appears an obvious decline with the decrease of PEG. As the intensity of absorption peak bases on the concentration of Ag NPs, it reflects a decline in

Ag NPs productivity of precursor solutions with the decrease of PEG. The black curve appears an absorption band at ca. 430nm, suggesting a large size of Ag NPs. When the ratio of PEG/EG decline to 2:1 the curve became sharp, and the absorption band blue shifted to ca. 400nm which was the shortest wavelength here, reflecting a small size and narrow distribution of Ag NPs, consistent with the result of size distribution histograms very well. With the decrease of PEG/EG (from 2:1 to 1:2) the absorption band gradually red-shift to 420nm, indicating an increase in average particle size. It must be noted when the ratio of PEG/EG declined to 1:5, the absorption band again blue-shifted. It seems that the particle size became small once again as talked above. But the productivity of Ag NPs is very low that is insignificance for practical application. If the synthesis was allowed to be proceeded, Ag NPs would grow larger out of control.

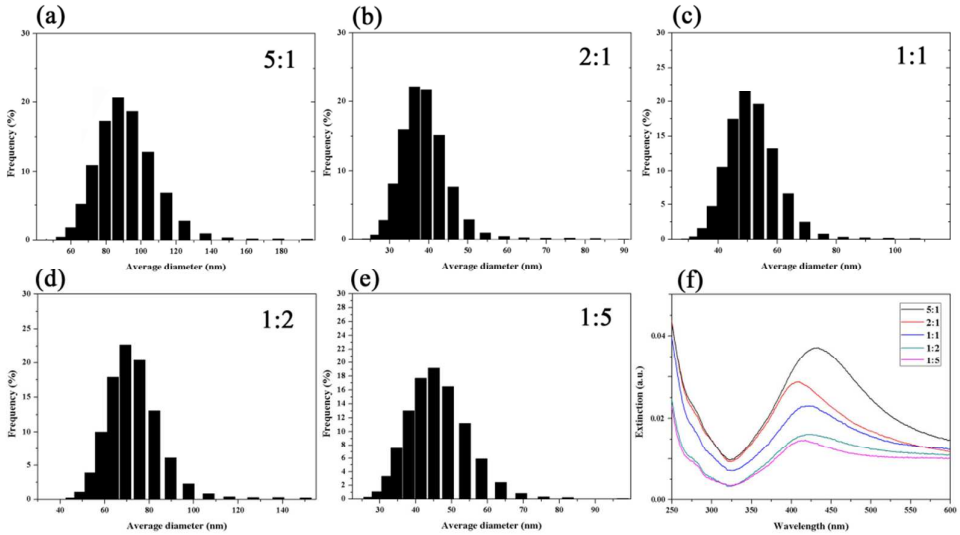

Fig. 2 (a-e) Size distribution histograms of Ag NPs taken from the samples listed in figure 1B (the ratio of PEG/EG were shown on the right top). (f) UV/vis spectra of ethanol dispersion of Ag NPs marked by the ratio of PEG/EG from 5:1 to 1:5.

Figure 3 illustrates the growth mode of Ag NPs respectively in EG and PEG, supposing the complete dissolution of reagents. In a typical synthesis of metal nanocrystals, a precursor compound is either decomposed or reduced to generate zero-valent atoms. These zero-valent atoms incline to assemble together immediately and form a cluster, i.e. nucleus of metal, which can be considered as a seed.[32] The nucleation course is based on the premise that the concentration of generated metal atoms has reached a point of supersaturation. Once formed, the seeds will continue to grow in an accelerated manner while the concentration of surrounded metal atoms in solution drops. If the concentration of atoms drops quickly below a level of minimum supersaturation, it is hard to generate new seeds any more. But with continuous supply of atoms produced by the precursor decomposition in low concentration, those original seeds can also in situ grow into larger nanocrystals, and it is only stopped by finishing all of the freshly generated atoms. It is not difficult to note that slow reaction rate favors the development of nanocrystal but not nucleation. During growth, some seeds and nanocrystals are prone to assemble together if the viscosity of solution is relatively low.[33] Hence in this point, the final size of Ag NPs mainly depend on the reducibility and viscosity of solvent. In our opinion, strong reducibility and high viscosity of solvent also benefit the balance between nucleation and crystallite growth, enhancing the productivity of monodisperse nanoparticles with small size. There is a competition between nucleation and crystallite growth. Nucleation continuously consumes plenty of freshly produced atoms which could obstruct the development of seeds. In additional to this, atoms also need some certain kinetic energy to transit a short pass in the solvent before they are captured by the seeds. Since the interaction between silver atoms and solvent molecular is stronger in higher viscosity solution such as PEG, it will take more energy for seeds to capture surrounding atoms; but the concentration of reduced atoms increases fast at the same time; many atoms, which do not be captured by seeds in time, will assemble together forming into new seeds. Therefore, high viscosity environment encumber the growth of silver nanocrystals.

It is worthwhile to discuss the aggregation and coalescence of nanocrystals during growth. These behaviors can also result in a large size of nanoparticle, and have a high incidence in low viscosity solution. Nanocrystals are much freer in low viscosity solution because of the weaker interaction between them and solvent molecules, more likely to collide and aggregate with each other. PEG owing high viscosity and strong reducibility is just proper for the size-controlled synthesis of Ag NPs. But it is hard to dissolve PVP and AgNO3 in PEG directly. So, here EG

was used for solvent firstly, then PEG was added to alter the viscosity and reducibility. When the ratio of PEG/EG reached ca. 2:1, homogenized solution of PVP and AgNO3 was prepared; and monodisperse small Ag NPs were produced in high yield.

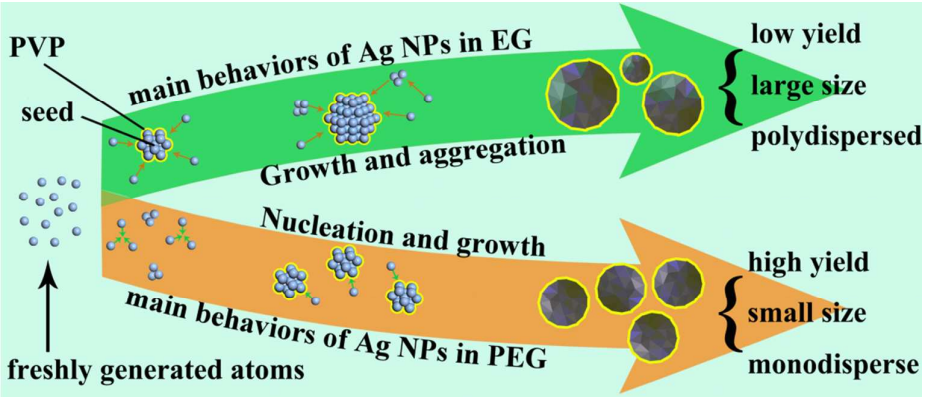

Fig. 3 Schematic illustration showing the growth behaviors of Ag NP respectively in EG and PEG, incurring different results.

The small particles have many advantages in preparing conductive inks which can be sintered at room temperature. Due to the small size, nanocrystals could be redispersed in various solvent preparing stable dispersion and could be sintered easily, leading to high conductive patterns. In order to investigate the performance of small Ag NPs in room temperature sintering, a contrast experiment was carried out between the large Ag NPs and the small ones during the sintering process. It must be noted that a spontaneous sintering realized by chemical process, which can be carried out at room temperature, has been employed in our experiment instead of conventional sintering by heating. We call it chemical sintering which will be amply discussed latter. Figure 4 shows serial SEM images of the two kinds of Ag NPs at different stages during chemical sintering. The sample shown in figure 4A was directly obtained by our previous method without using PEG.[29] The detail of a typical particle was shown by the HR-TEM image (the inset of figure 4A). By contrast, the small Ag NPs shown in figure 4a were prepared with the current method with the ratio of PEG/EG at 2:1. The inset HR-TEM image also shows a typical particle which is co. 30nm in diameter. Both of the two Ag NPs are spherical in shape; and the large one seems with fewer defects on it. The sintering procedure was allowed to proceed for ca. 90 min. There were not significant changes happed to the large Ag NPs (figure 4A-E). It was only observed that the skeleton of the Ag NPs shrank into high density structure. The level of coalescence seems very low; even after 90 min's sintering, many individual particles could be observed clearly.

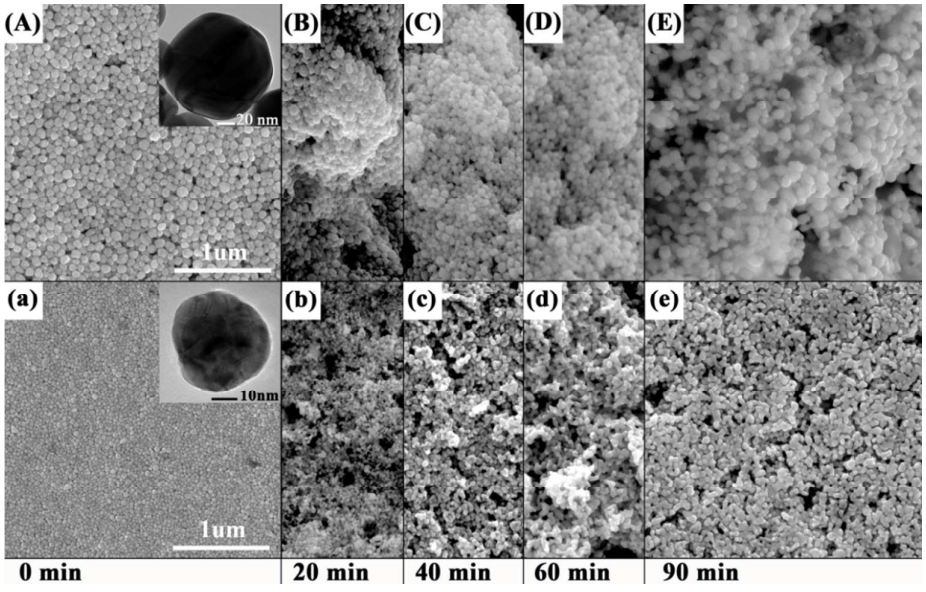

Fig. 4 A series of SEM images of two kinds of Ag NPs (large and small in average size) taken during the chemical

sintering process. (A-E) The large Ag NPs obtained through our previous approach without participation of PEG. (a-e) Size-controlled Ag NPs prepared by the current method with a ratio of PEG/EG at 2:1.

Contrarily, a dramatic change has happened to the small Ag NPs during chemical sintering. Most of the small Ag NPs aggregated in ca. 20 min. After another 20 min, crystal growth and particle coarsening became obvious; some huge clusters generated which are many times larger than the original particles. When the sintering was proceeded to 60 min, most of the particles have coalesced together; some blocky structures were also developed. The microstructure was almost fixed after sintering for ca. 90 min. Though it was still a porous structure, there were hardly any individual particles. The intergranular neck formation and grain growth between particles became more complete that could make the structure high conductive.

Why it could be sintering at room temperature? The mechanism of chemical sintering is worthwhile to be investigated. It is a complicated process which is triggered by the detachment of PVP (i.e. the capping agent) from the surface of Ag NPs with some anions such as Cl^-, HS^-, S^{2-}, ect. Those anions were evaluated in our experiment as the desorbing agent for PVP; and Cl^- performed better than the others, hence it was chosen in this report. The deposition phenomenon of Ag NPs as shown in figure 5a may explain the effectiveness of HCl in detachment of PVP which is beginning of chemical sintering. It can be seenthat one of the samples has suffered a deposition in 90min after injection of HCl, indicating the Ag NPs became unstable in the presence of HCl. Figure 5d shows the UV/vis spectra of the sample recorded during the deposition course respectively at the time of 0, 45 and 90 min. The intensity of the major peaks presented a decline tendency during the deposition, indicating a decrease in the concentration of dispersed Ag NPs. The peaks also appeared a slight red-shift from ca. 400 to 410 and 415 nm, which may be caused by the increase on particle size. The broadened peaks suggested a wide distribution in particle size; and this conclusion is consistent with the histograms of Ag NPs very well (figure 5e-g).

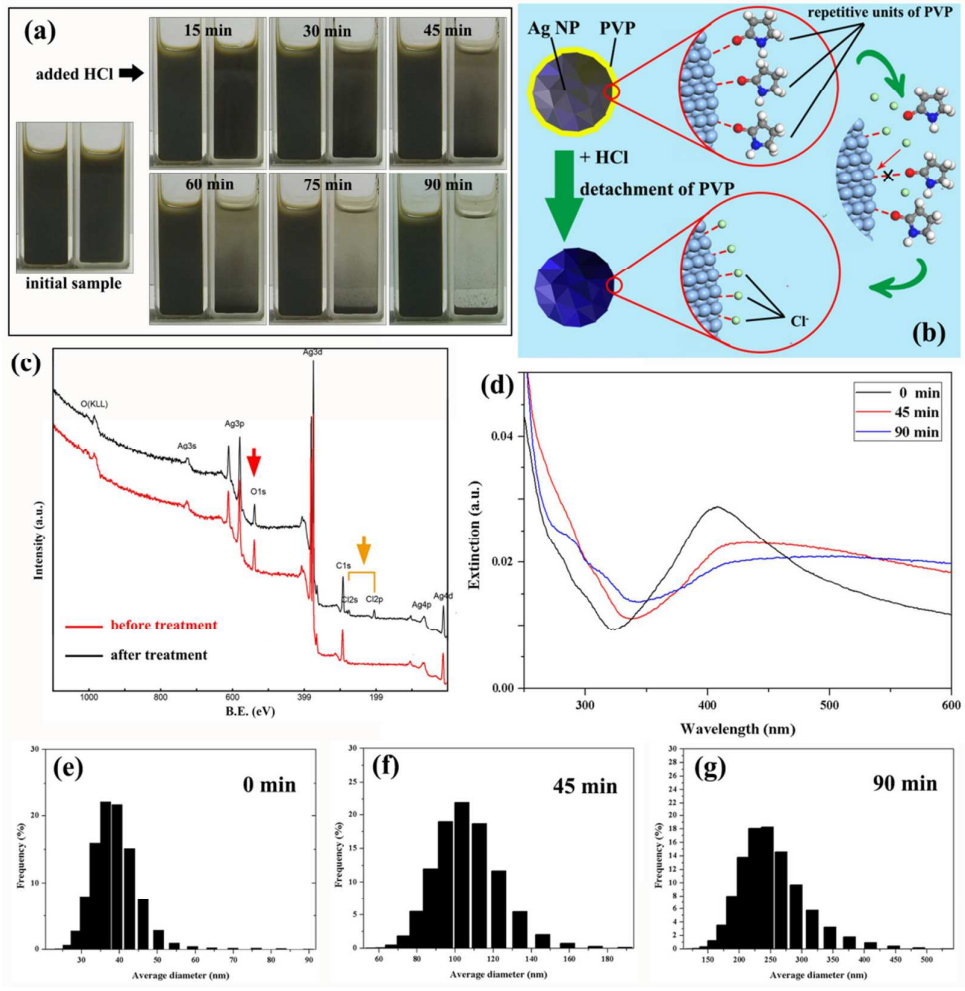

Fig. 5 Evidences on detachment of PVP and schematic illustration. (a) Deposition of the small Ag NPs caused by injection of HCl into the dispersion. (b) Schematic illustration of the detachment of PVP by Cl^- from the surface of Ag NPs. (c) XPS spectra of Ag NPs that were taken respectively before and after the treatment. (d) Changes on

UV/vis spectra of the dispersion of small Ag NPs after injecting HCl; the samples were diluted 1000 times with ethanol before characterization. (e-g) Particle size distribution of Ag NPs at the three stages of the treatment.

Figure 5c shows the XPS spectra of the powder sample of Ag NPs which were obtained respectively before and after the treatment. It could be found that the O 1s binding energy has been weakened and Cl 2s and 2p appeared on the XPS profiles after treatment. It is believed that this result is caused by the detachment of PVP from the surface of Ag NPs with Cl^-; and a probable mechanism was illustrated by figure 5b. It was no doubt that PVP adsorbs on the surface of Ag NPs through the oxygen of the carbonyl group of the pyrrolidone ring.[34-37] The desorption may be possible by substituting the carbonyl group with Cl^- on the same sit. The changes on XPS spectra also support this explain. As there was no capping agent, the Ag NPs were prone to aggregate together forming some large clusters and settling down. Then it was followed by a spontaneous sintering process involving complex transformation of crystalline structure.[38]

The spontaneous sintering in fact is crystal growth or particle coarsening process which could just consolidate nanoparticles together, leading to a consequence which is similar to sintering at high temperature. On the top of figure 6, it shows two major processes of coarsening which not only lead to the growth of aggregated Ag NPs but also combine them together. Coalescence occurs when two nanocrystals collide and merge together developing into one big nanocrystals.[39] It usually needs relative high energy which may come from system such as high surface energy or from environment such as by heating. Ostwald ripening occurs by evaporation of atoms from one nanocrystals, which then transfer to another.[30] It is a spontaneous dynamic process, both nanocrystals exchange atoms, but the rate of loss from the smaller ones is higher because of the lower average coordination of atoms at the surface and relative ease of removal. Thus big nanocrystals grow bigger at the expense of small ones as nutrient, which shrink and eventually disappear.

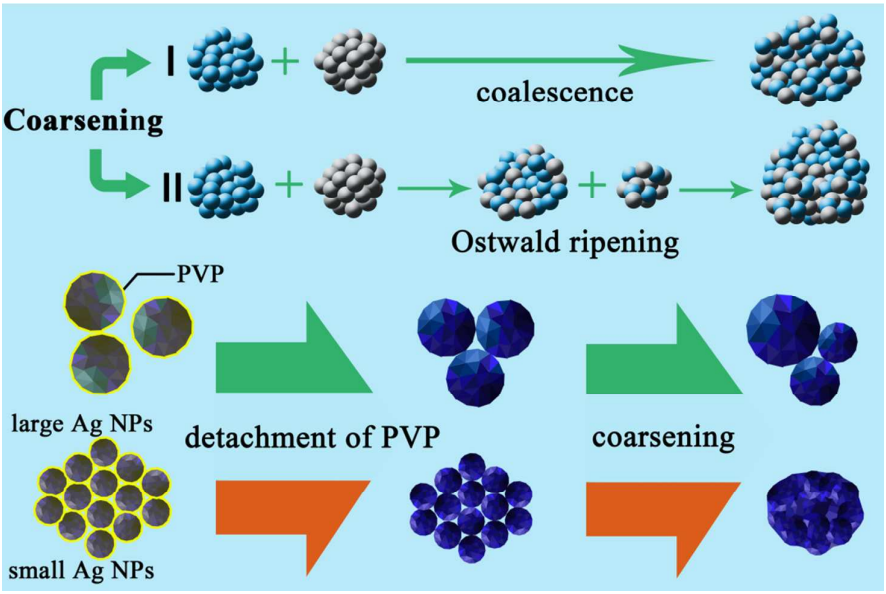

Fig. 6 Schematic illustration of the difference between the large Ag NPs and the small ones during chemical sintering. Coarsening is an irreversible procedure whereby clusters or nanoparticles increase their size and reduce their number. Two main mechanisms are shown here: Ⅰ, coalescence process, and Ⅱ, Ostwald ripening process. Both two behaviors are prone to happen during chemical sintering of the small Ag NPs, but hard for the large ones.

As shown at the bottom of figure 6, when the detachment of PVP has been finished, it is followed by a spontaneous sintering process as soon as the naked Ag NPs contact each other. The large particles, duo to their relative perfect crystal texture and high stability, they need higher energy to reform and eliminate the interface between them, hence hard to coalesce together directly. But unlike bulk material the large particles are still nanocrystals, which have high specific surface areas. The atoms on the surface of particles are more energetically unstable than those within. Therefore the unstable surface atoms often migrate between particles to seek more stable place over time. Those relative larger particles, owning higher average coordination of atoms, are prone to accommodate those free atoms leading to a growth in their size by consuming other smaller particles. This coarsening mainly relies on Ostwald ripening. Chemical sintering seems harder for the large particles; as shown in figure 4E, many individual particles were left after sintering. By contrast, the small Ag NPs have higher specific surface being less stable and tend to agglomerate due to the high surface tension, which perform well in the

chemical sintering. Both coalescence and Ostwald ripening could easily occur during this process. Those behaviors make the structure of small Ag NPs more compact and integrity (figure 4e). It could be note that many voids inevitably generated in the sintering, caused by the detachment of PVP that shrank the framework of Ag NPs. Since the small particles have higher mobility and space occupation, these voids may be filled up gradually; hence more compact and solid silver patterns could be fabricated by small Ag NPs.

In order to investigate the further advantages of small Ag NPs in fabricating conductive patterns, more characterizations were carried out to compare the quality and conductivity of silver patterns that were fabricated with large and small Ag NPs respectively. Figure 7a shows the XRD patterns of the powder samples of Ag NPs respectively before and after chemical sintering. The five peaks on the diffraction profile at 2θ of 37.9°, 44.1°, 64.2°, 77.2° and 80.9° are respectively indexed as (111), (200), (220), (311) and (222) (JCPDS file No. 04-0783) reflections of the face-centered cubic (fcc) structure of silver. Obviously, the tendency of all the peaks became stronger after chemical treatment; and the peaks slightly became narrower and sharper, indicating that a grain growth has occurred during the treatment, resulting in a high degree of crystallinity. Grain growth not only decreases the density of deformation and twin faults but also enlarges the crystallite in size.[38] And crystallite size was evaluated by the Debye-Scherrer equation, Dhkl=Kλ/Bhklcosθ (Dhkl is the crystallite size; λ is the wavelength of the X-ray; Bhkl is the full-width at half-maximum of the diffraction peak; θ is the Bragg angle).[40] The result shows the large Ag NPs have an increase from ca. 23 to 52 nm in size; and the size of small ones has increased from ca. 19 to 65 nm. It seems that all the calculated sizes are smaller than those observed by SEM or detected by laser diffraction particle size analyzer. But in our opinion, there is no contradiction. The reason lies on that the Ag NPs are polycrystalline subgrains. A subgrain can contain several crystallites; Debye-Scherrer equation merely estimates the size of crystallite, hence the calculated volume is smaller than observed.[41] Here we could note the increase on size is more excellent for the small Ag NPs according to calculation, indicating that chemical sintering favors small particles, consistent with the preceding results very well.

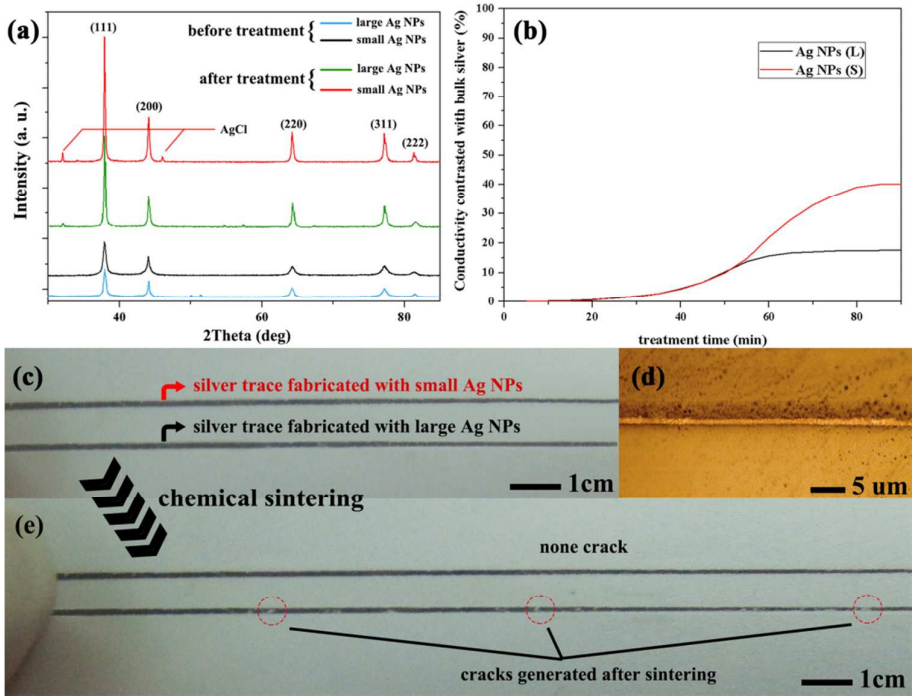

Fig. 7 (a) X-ray diffractions of the two types of Ag NPs taken by powder samples which were respectively obtained before and after chemical sintering. (b) The relationship between the conductivity of the two samples and chemical sintering time (using conductivity of bulk silver as reference). (c) Photo of the two silver traces respectively fabricated with the large and the small Ag NPs. (d) Microsection image of a typical vertical section of the silver traces. (e) Photo of the same silver traces shown in figure7c which were taken after 90 min's chemical sintering.

It could be noted on the XRD spectrum profiles patterns of the sintered samples, two weak peaks marked with red lines at 32.0° and 46.0° were assigned to the diffraction of the (111) and (200) crystal planes of the fcc AgCl (JCPDS file No. 31-1238), suggesting that after the chemical sintering had proceeded for 90 min a small amount of silver existed in AgCl. Associating the result with XPS spectra, it could be inferred that some AgCl were formed at

the stage of detaching PVP; some Cl^- may bond to the surface of Ag NPs as a substitute for PVP. We were interest in whether this phenomenon would fail the electrical conductivity of printed patterns after chemical sintering, hence a contrast was made between the two kinds of Ag NPs. Silver traces were fabricated on FR-4 substrate respectively using the dispersions of large Ag NPs and the small ones as shown in figure 7c. A typical vertical section of these traces were showed by the microsection image (figure 7d). It can be judged that those silver traces are ca. 1 mm in width and ca. 1 um in thickness. The pattern was treated in 0.1M HCl at room temperature for 90 min; after each 5 min, it was taken out, washed, dried to record the resistivity. In order to facilitate comparison of the conductivities between the two silver traces over time, the relation curves between conductivity and sintering time as shown in figure 7b were drawn according to these data. Obviously, resistivity of silver trace was infinity before sintering; even though Ag NPs were compactly deposited on the substrate, there was PVP capping layer between them acting as an insulated barrier. As soon as PVP was detached, direct surface contact of particles was established, allowing a trickle of electric current to pass through. When the sintering proceeded for ca. 20 min, there appeared a rapid decrease in resistivity, bringing a conductivity even closed to semiconductor. In this period, the decline in resistivity is mostly attributed to the shrink on the framework of Ag NPs caused by the detachment of most PVP, enabling a deep contact between particles. The sample fabricated with large Ag NPs gradually lost its dominance in conductivity since the chemical sintering have been proceeded for ca. 40 min. Referring to figure 4, no manifest changes has happened to the structure of large Ag NPs because of an incomplete chemical sintering as discussed above. Coalescence, Ostwald ripening and grain growth are slow process, but can generally reduce the density of defects, refining the crystal texture and really combining particles into one body. Small Ag NPs were benefited from those behaviors during the second half of chemical sintering; hence, more compact and solid structure was obtained after treatment, presenting a high conductivity even up to ca. 40% that of bulk silver.

There was another phenomenon, which occurred in the chemical sintering, attracted our attention. It can be seen in figure 7e that some pieces of silver trace fabricated with the large Ag NPs were shed after the treatment, appearing some cracks on the pattern. The reason lies on the relative poor adsorption of the large Ag NPs to the substrate. Voids generated by detachment of PVP would never be filled up due to the lower space utilization of large particles, loosening the structure; the incomplete chemical sintering has not largely merged particles together. Therefore, the patterns fabricated with large Ag NPs were prone to be shed in ultrasonic treatment. Once again the small Ag NPs performed better in adhesion to substrate and stood the whole chemical sintering without cracks. Duo to those superiorities, it is believed that this small Ag NPs would have extensive applications in flexible and plastic electronics, especially for preparing conductive inks which could be printed on temperature sensitive substrates.

Conclusions

In summary, monodisperse Ag NPs of ca. 37nm in diameter were successfully produced in high yield with the participation of PEG in a typical polyol process. These small size Ag NPs are proper for the production of conductive inks which could be conveniently used to fabricate high conductive subtle silver trace at room temperature on many substrates due to their superiority in the chemical sintering. The small Ag NPs are more prone to merge together leading to a grain growth by the behaviors of coalescence and Ostwald ripening in chemical sintering, which is triggered by the detachment of capping agent, i.e. PVP. After chemical sintering, the small particles formed a solid and compact structure and exhibited high conductivity in printed patterns. The conductivity obtained by room temperature sintering has reached ca. 40% of the conductivity of bulk silver; in addition, these Ag NPs have better adhesion to substrates than the previous larger ones, making us believe that they would have extensive applications in the technology of printed electronics.

Acknowledgements

This work is supported by the Major Scientific and Technological Projects of Guangdong Province (2011A090200017) and National Natural Science Foundation of China [Supported by NSFC (No：61240055)].

Notes and reference

State Key Laboratory of Electronic Thin Films and Integrated Devices, University of Electronic Science and Technology of China, No.4,Section 2,North Jianshe Road, Chengdu, Sichuan, P.R.China. ZIP: 610054; Fax: +86-28-832 03218; Tel: +86-28-832 03218; E-mail: heweiz@uestc.edu.cn; tangyao2003@163.com

1 H. M. Nur, J. H. Song, J. R. G. Evans and M. J. Edirisinghe, J. Mater. Sci. Mater. Electron. 2002, **13**, 213
2 J. T. Wu, S. L. C. Hsu, M. H. Tsai and W. S. Hwang, J. Phys. Chem. C 2010, **114**, 4659
3 K. Woo, D. Kim, J. S. Kim, S. Lim and J. Moon, Langmuir 2009, **25**, 429
4 S. Jeong, H. C. Song, W. W. Lee, S. S. Lee, Y. Choi, W. Son, E. D. Kim, C. H. Paik, S. H. Oh and B. H. Ryu, Langmuir 2011, **27**, 3144
5 A. Denneulin, J. Bras, A. Blayo, B. Khelifi, F. R. Dherbey and C. Neuman, Nanotechnology 2009, **20**, 385701
6 A. Denneulin, J. Bras, F. Carcone, C. Neuman and A. Blayo, Carbon 2011, **49**, 2603

7 R. Sangoi, C. G. Smith, M. D. Seymour, J. N. Venkataraman, D. M. Clark, M. L. Kleper and B. E. Kahn, J. Disper. Sci. Technol. 2004, **25**, 513
8 K. F. Teng and R. W. Vest, Electron Device lett. IEEE 1988, **9**, 591
9 J. F. Mei, M. R. Lovell and M. H. Michle, Electron. Packag. Manuf. IEEE 2005, **28**, 265
10 J. D. Newman and A. P. F. Turner, Anal. Chim. Acta 1992, **262**, 13
11 B. Comiskey, J. D. Albert, H. Yoshizawa and J. Jacobson, Nature 1998, **394**, 253
12 W.Dungchai, O.Chailapakul and C. S. Henry, Anal. Chem. 2009, **81**, 5821
13 V. Lakafosis, A, Rida, R. Vyas, Y. Li, S. Nikolaou and M. M. Tentzeris, Proc. IEEE 2010, **98**, 1601
14 A. Rida, Y. Li, R. Vyas, and M. M. Tentzeris, Anten. Propag. Mag. IEEE 2009, **51**, 13
15 S. Jeong, H. C. Song, W. W. Lee, Y. Choi and B. H. Ryu, J. Appl. Phys. 2010, **108**, 102805
16 J. Perelaer, C. E. Hendrinks, A. W. M. Laat and U. S. Schubert, Nanotechnology 2009, **20**, 165303
17 J. T. Wu, S. L. C. Hsu, M. H. Tsai and W. S. Hwang, J. Phys. Chem. C 2011, **155**, 10940
18 S. C. Hung, O. A. Nafday, J. R. Haaheim, F. Ren, G. C. Chi and S. J. Peraton, J. Phys. Chem. C 2010, **114**, 9672
19 R. Zhang, W. Lin, K. Moon and C. P. Wong, ACS Appl. Mater. Inter. 2010, **2**, 2637
20 S. B. Walker and J. A. Lewis, J. Am. Chem. Soc. 2012, **134**, 1419
21 C. L. Lee, K. C. Chang and C. M. Syu, Coll. and Surf. A: Physico. and Eng. Aspects 2011, **381**, 85
22 J. Perelaer and B. J. Gans, Adv. Mater. 2006, **18**, 2101
23 J. Perelaer, M Klolkkenburg, C. E. Hendriks and U. S. Schubert, Adv. Mater. 2009, **21**, 4830
24 S. H. Ko, H. Pan, C. P. Grigoropoulos, C. K. Luscombe, M. J. Fréchet and D. Poulikakos, Appl. Phys. Lett. 2007, **90**, 141103
25 M. Hummelgård, Z. Zhang, H. Nilsson, O. Håkan and D. Aristides, Plos ONE 2011, **6**, e17209
26 M. L. Allen, M. Aronniemi, T. Mattila, A. Alastalo, K. Ojanperä, M. Suhonen and H. Seppä, Nanotechnology 2008, **19**, 175201
27 S. Magdassi, M. Grouchko, O. Berezin and A. Kamyshny, ACS Nano 2010, **4**, 1943
28 M. Grouchko, A. Kamyshny, C. F. Mihailescu, D. F. Anghel and S. Magdassi, ACS Nano 2011, **5**, 3354
29 Y. Tang, W. He, G. Zhou, S. Wang, X. Yang, Z. Tao and J. Zhou, Nanotechnology 2012, **23**, 355304
30 S. R. Challa, A. T. Delariva, T. W. Hansen, S. Helveg, J. Sehested, P. L. Hansen, F. Garzon and A. K. Datye, J. Am. Chem. Soc. 2011, **133**, 20672
31 R. Ouyang, J. X. Liu and W. X. Li, J. Am. Chem. Soc. 2013, **135**, 1760
32 V. K. LaMer and R. H. Dinegar, J. Am. Chem. Soc. 1950, **72**, 4847
33 M. A. Watzky, R. G. Finke, J. Am. Chem. Soc. 1997, **199**, 10382
34 Y. Gao et al. J. Phys. Chem. B 2004, **108**, 12877
35 P. S. Mdluli, N. M. Sosibo, N. Revaprasadu, P. Karamanis and J. Leszczynski, J. Mol. Struct. 2009, **935**, 32
36 P. S. Mdluli, N. M. Sosibo, P. N. Mashazi, T. Nyokong, R. T. Tshikhudo, A. Skepu and E. Lingen, J. Mol. Struct. 2011, **1004**, 131
37 W. A. Al-Saidi, H. Feng and K. A. Fichthorn, Nano Lett. 2012, **12**, 997
38 B. Ingham, T. H. Lim, C. J. Dotzler, A. Henning, M. F. Toney and R. D. Tilley, Chem. Mater. 2011, **23**, 3312
39 M. Grouchko, I. Popov, V. Uvarov, S. Magdassi and A. Kamyshny, Langmuir 2009, **25**, 2501
40 U. Holzwarth and N. Gibson, Nanotechnology 2011, **6**, 534
41 T. Ungár, J. Gubicza, G. Ribárik and A. Borbély, J. Appl. Cryst. 2001, **34**, 298

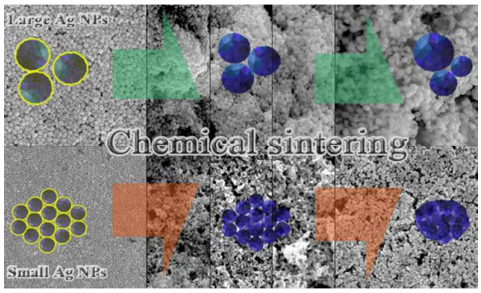

Silver nanoparticles with controlled size present high conductivity after room temperature sintering achieved by a chemical process.